

Protein Identity and Environmental Parameters Determine the Final Physico-Chemical Properties of Protein-Coated Metal Nanoparticles

Inna Dewald, Olga Isakin, Jonas Schubert, Tobias Kraus, and Munish Chanana

The Journal of Physical Chemistry C

This document is the unedited Author's version of a Submitted Work that was subsequently accepted for publication in *The Journal of Physical Chemistry C*, copyright © American Chemical Society after peer review. To access the final edited and published work see <http://dx.doi.org/10.1021/acs.jpcc.5b06266>.

Protein Identity and Environmental Parameters Determine the Final Physico-Chemical Properties of Protein-Coated Metal Nanoparticles

Inna Dewald,^{a,†} Olga Isakin^{a,†} Jonas Schubert,^a Tobias Kraus,^b Munish Chanana^{a,c,}*

a Physical Chemistry II, University of Bayreuth, 95447 Bayreuth, Germany

b INM – Leibniz-Institut for New Materials, 66123 Saarbrücken, Germany

c Institute of Building Materials (IfB), ETH Zurich, 8093 Zurich, Switzerland

* corresponding author, munish.chanana@uni-bayreuth.de

† authors contributed equally

Abstract

When a nanomaterial enters a biological system, proteins adsorb onto the particle surface and alter the surface properties of nanoparticles, causing drastic changes in physico-chemical properties such as hydrodynamic size, surface charge and aggregation state, thus giving a completely new and undefined physico-chemical identity to the nanoparticles. In the present work, we study the impact of the protein identity (molecular weight and isoelectric point) and the environmental conditions (pH and ionic strength) on the final physico-chemical properties of a model nanoparticle system, i.e. gold nanoparticles. Gold nanoparticles either form stable dispersions or agglomerate spontaneously when mixed with protein solutions, depending on the protein and the experimental conditions. Strikingly, the agglomerates redisperse to individually dispersed and colloidally stable nanoparticles, depending on the purification pH. The final protein coated nanoparticles exhibit specific stabilities and surface charges that depend on protein type and the conditions during its adsorption. By understanding the interactions of nanoparticles with proteins under controlled conditions, we can define the protein corona of the NPs and thus their physico-chemical properties in various media.

Introduction

Safe use of nanomaterials in industrial and life science applications requires to fundamentally understand and to control the interactions of nanomaterials with biological systems.¹⁻⁷ These interactions strongly depend on the physico-chemical properties of the nanomaterial (including colloidal stability, surface charge and wettability) and the physiological parameters in the biological system. In cells and organisms, the situation becomes complex, because the environmental conditions (such as pH, ionic strength, temperature) and composition (presence of various solutes and biomolecules) can differ from compartment to compartment.⁷ When a nanomaterial enters a biological system, its surface is immediately covered by biomatter, usually proteins.¹⁻² Proteins adsorb onto the particle surface forming an undefined protein 'corona'.³⁻⁶ The adsorbed proteins alter the surface properties of nanoparticles (NPs), cause drastic changes in the physicochemical properties such as hydrodynamic size, surface charge and aggregation state, and give a new and unknown physico-chemical identity to the NPs. This physico-chemical identity determines the particles' fate in biological systems mediated by their interaction with biomolecules and membranes in various physiological environments.⁷ Deeper understanding of the nuances of NP bonding within biological environments is required to advance their applicability in life science applications, but also to foresee their long-term fate in human body and environment.² Here, we investigate the interactions of NPs with proteins under controlled conditions to ultimately describe, explain, and control the protein corona of the NPs and thus their final physico-chemical properties.

Gold NPs in combination with proteins have been used as colorimetric detectors of proteins,⁸⁻¹⁰ to study proteins' structural conformation,^{9, 11} protein kinetics^{10, 12} and their chemical modifications.^{9, 13} In terms of medical applications, they have been used as specific targets and for the delivery of drugs and biomolecules.¹⁴⁻¹⁶ In all of these applications, it is paramount to maintain the stability of colloidal gold solutions by suppressing aggregation. Stability depends on the interplay of a) the nanoparticle surface chemistry (*nanoparticle*

identity), b) the properties of the protein (*protein identity* i.e. molecular composition, molecular weight (MW), isoelectric point (pI), folding) and c) environmental parameters (*environmental identity*, i.e. solvent, pH, ionic strength, temperature). For example, gold NPs have been mixed with proteins such as bovine serum albumin (BSA), human serum albumin (HSA), ovalbumin (Ova), insulin (Ins), β -lactoglobulin (BLG), lysozyme (LYZ), and trypsinogen (Tg).¹⁷⁻¹⁹ Depending on the *protein identity* (pI and MW) and the experimental conditions (*environmental identity*: pH, concentrations, ionic strength), either stable particle dispersions¹⁸⁻²⁰ or particle aggregates^{17-19, 21-22} are obtained, which can easily be demonstrated in the case of gold NPs by the color change of dispersions. The aggregation process can be easily monitored by the shift and broadening of the LSPR band.

Proteins are usually dissolved in pH controlled buffer solutions (phosphate^{17, 23-24} TRIS,²³ borate,²³ hepes²⁴ or at physiological conditions (pH 7.4)), and effects of the ionic strength and pH of the media have to be considered. For example, Chen et al.¹⁸ mixed a series of proteins such as ribonuclease A (Rib), cytochrome C (cyt C), Tg, α -chymotrypsinogen A (α -Chy), myoglobin (Myo), hemoglobin (Hb), Conalbumin (CA), α -lactalbumin (α -Lac), Ova, BSA, β -casein (β -Cas), glucose oxidase (GO), and Ins with citrate-coated gold NPs (Au@Citrate) in 10 mM glycine at pH 7 and observed immediate aggregation for all the high-pI proteins, including Hb. They suggested the electrostatic interactions between the positively charged proteins and the negatively charged NPs to cause agglomeration. On the other hand, Garabagiu et al.¹⁹ mixed Hb with Au@Citrate NPs in 100 mM phosphate buffer and observed strong binding of Hb without signs of aggregation. Hydrophobic interactions were invoked to explain adsorption. A recent study²⁵ revealed that Au@Citrate NPs agglomerate in the presence of Hb at acidic pH (pH 4), but in different manners, depending on the ratio between the NPs and the protein. Depending on the concentration ratio [Hb]/[Au@Citrate], the mixture remained stable, agglomerated and precipitated, or formed stable dispersions of hybrid AuNP:Hb clusters. It was suggested that agglomeration was caused either by particle bridging or by electrostatic destabilization from the oppositely charged Hb and sufficiently high protein concentrations lead to the formation of stable particles and clusters.²⁵

We previously reported on extremely stable, protein-coated gold NPs (Au@Protein NPs)²⁶⁻²⁸ and gold nanorods.²⁹ We were able to adsorb moderate-pI proteins such as Ins, BSA, BLG and Ova onto gold NPs of different surface chemistries.²⁶⁻²⁹ The resulting particles exhibited extremely high colloidal stability, and reversible agglomeration/disagglomeration behavior indicated strong binding of proteins to the gold surface. Although indications about the interrelationship between the *nanoparticle identity*, *protein identity* and the *environmental identity* exist,^{23, 30} a systematic study of the interactions between Au(metal) NPs and proteins has not been reported so far. In this study, we seek to understand what governs the interactions of proteins with Au NPs, to describe and explain the mechanisms of protein corona formation, and to ultimately control the physico-chemical properties of Au@Protein NPs.

Nanoparticle identity comprises the particle size, shape, core material and coating material. The first two can be adjusted precisely during the synthesis of the nanomaterials. Core material and coating material define the surface chemistry and the interfacial properties of the particles that are relevant for the interactions between proteins and particles and the adsorption of proteins to the particle surface. From the plethora of various types of organic and inorganic particles consisting of polymers such as latex,³¹ hydrogels,³² oxides (Fe₃O₄, SiO₂),³³ sulfides (CdTe/CdS, ZnS),³⁴ or metal NPs, AuNPs qualify particularly well for studying such interactions because of their plasmonic properties. They exhibit a localized surface plasmon resonance (LSPR) band, which can be excited in UV-Vis-NIR spectral range. The LSPR is highly sensitive to size, shape and inter-particle distance and depends on the refractive index of the surrounding media. The sensitivity of the NPs to the changes in surrounding medium and the inter-particle distance has been used as optical tool for detecting material adsorption events³⁵⁻³⁶ and aggregation events induced by the material adsorption to particles.²⁵

Nearly all types of NPs bear organic coatings during and after the synthesis, such as small charged molecules, surfactants or polymers, which are essential for the size and shape control but also for their colloidal stability. For studying the adsorption interactions of proteins onto NPs, it is reasonable to use NPs that bear neither stealth coatings (e.g. PEG)³⁷ nor coatings such as surfactants (e.g. CTAB)³⁸ that interact with proteins, and thus distort the protein-particle interactions ambiguously. Citrate has proved to be a versatile and simple stabilizing agent for various types of NPs, including metal and metal oxide NPs. The negatively charged citrate shell with its large, negative ζ -potential (- 35 mV) sufficiently stabilizes the particles via electrostatic repulsion, preventing particle aggregation. Citrate binds weakly enough to the particle surface and therefore can be easily replaced with macromolecules, allowing for subsequent surface functionalization with surfactants, polymers and even proteins.

The *protein identity* is the other essential in the interactions of proteins with NPs. The intrinsic properties of proteins differ from species to species, depending on their biological function. Proteins differ in their molecular weights, isoelectric point, and display different domains, which can be negatively or positively charged or even hydrophobic, depending on their chemical composition and 3D-structure. Thus, different proteins may interact differently with the same kind of NPs.

For the electrostatic interactions between proteins and NPs the charge of the protein and that of NPs will play a significant role, which of course depends on the environmental parameters such as pH, ionic strength and temperature of the dispersion media. Hence, for properly studying the protein particle interactions, the *environmental identity* of the system has to be carefully selected as well.

Herein, we systematically studied the impact of two parameters, *protein identity* and *environmental identity*, on the colloidal stability of protein-coated NPs and on the robustness of the final protein corona, while keeping the third parameter, *nanoparticle identity*, constant.

Experimental Section

Chemicals: Gold(III) chloride trihydrate ($\geq 99.9\%$), trisodium citrate dehydrate ($\geq 99.9\%$), phosphate buffered saline (PBS), conalbumin type I from chicken egg white (CA), β -lactoglobulin from bovine milk (BLG), Lysozyme from chicken egg white (LYZ), pepsin from porcine gastric mucosa (Pep), bovine serum albumin (BSA), human hemoglobin (Hb), ovalbumin from chicken egg white (Ova), cytochrom C from bovine heart (cyt C), recombinant human insulin (Ins), and trypsinogen from bovine pancreas (Tg), were purchased from Sigma-Aldrich. All chemicals were used as received. MilliQ water (18.2 M Ω .cm) was used in all aqueous solutions. The pH was adjusted using 0.1 M or 1 M HCl and NaOH from Grüssing.

Synthesis of Au@Protein NPs: Citrate-coated gold NPs (Au@Citrate) were synthesized by the Turkevich method³⁹ and used as synthesized. The average particle size was $d_{\text{TEM}} \sim 15$ nm, ($\lambda_{\text{max}} = 520$ nm; $d_{\text{DLS}} \sim 19$ nm; ζ -potential ~ -35 mV). The NPs were functionalized with proteins by a ligand exchange reaction as previously reported.²⁶⁻²⁸ Typically, 20 mg of a protein were dissolved in 2 mL of a 1 wt% citrate solution (\sim pH 7.4). The pH was adjusted to 2 and 12 with 1 M HCl and NaOH, respectively. Subsequently, 20 mL of citrate coated gold NPs solution ($[\text{Au}] = 0.26$ mM) were added to the protein solution in a shot. The mixture was stirred overnight (ca. 16 h) at room temperature. Finally, the protein coated gold NPs (Au@Protein) were purified and concentrated via 3-fold centrifugation (10 000 rcf, 20-30 min) using Milli-Q water with pH adjusted to 2, 7 and 12, and stored in the fridge at $\sim 7^\circ\text{C}$.

Characterization Techniques: All gold NP dispersions were characterized by means of the following techniques: UV-Vis absorption spectra were measured with a Specord[®]250 Plus spectrophotometer (Analytik Jena), the NP diameter (average of 3 measurements and 15 runs each) and ζ -potential (from the electrophoretic mobility at 25°C, average of at least 5

measurements and 10 - 50 runs each) were monitored using a Nano-Zetasizer (Malvern Instruments Co, Worcestershire, UK). Transmission Electron Microscopy (TEM) was carried out on EM 922 Omega (Zeiss) transmission electron microscope. The average NP size was calculated from at least 150 particles. In addition, Cryo-TEM measurements were performed at - 179°C and a pressure of 10⁻⁷ - 10⁻⁸ h Pausing a Zeiss/LEO EM 922 Omega (Zeiss NTS GmbH, Oberkochen, Germany). The pH values were measured by a digital pH meter Lab 850 (Schott® Instrument, SI Analytics GmbH).

Results and Discussion

In order to demonstrate the effect of the interplay of the three parameters, spherical Au@Citrate NPs of an average size of ~ 15 nm in diameter (**Figure S1** in the supporting information (SI)) were mixed with proteins of different pI and molecular weights dissolved in water (Milli-Q, no salt, pH 5-6) and in phosphate buffer saline (PBS, ionic strength 150 mM, pH 7.4). The Au@Citrate NP dispersions were added in one shot to relatively highly concentrated protein solutions (10 mg/mL, i.e. 1 wt%) in a volume ratio of 10:1, resulting in a final protein concentration of 1 mg/mL in the mixture. High protein concentrations were chosen to avoid particle aggregation due to bridging interactions, which usually occur at low protein or polymer concentrations.^{25, 33, 40} All experiments were performed at room temperature. The stability and the degree of agglomeration was judged by the red shift of the plasmon peak via UV-Vis and by hydrodynamic size measurements via DLS.

Figure 1 illustrates the protein-dependent behavior of the AuNPs dispersions. In water (**Figure 1A**), the very low-pI protein pepsin (Pep, negatively charged), the very high-pI proteins such as Tg, cyt C and LYZ⁴¹ (positively charged) and the neutral pI proteins such as CA and Hb caused a spontaneous agglomeration (**Figure 1C**) and fast precipitation (within 3 hours, data shown after 24 hours) of the NPs upon mixing. Stable NP dispersions are only

achieved for intermediate pI proteins (**Figure 1A, C**) such as Ova⁴², BSA⁴³⁻⁴⁴ and BLG⁴⁵ (negatively charged at the given pH values), except Ins.

The reason for the fast agglomeration of the negatively charged Au@Citrate NPs with the positively charged high pI-proteins (Tg, cyt C and LYZ) is assumed to be the strong electrostatic attraction forces between the NPs and the proteins.^{17-18, 25} For the neutral pI-proteins (CA and Hb) and Ins the effect may originate from the low solubility of the proteins in the absence of salt or due to the slightly acidic pH of the MilliQ water (pH 5-6), which is close to the pI of the proteins (Ins, CA). The increased solubility of proteins in the presence of salt at an optimum of salt concentration is known as the “salting in” effect.⁴⁶⁻⁴⁷ The effect of salt concentration can be seen in **Figure 1B**. The proteins Ins, CA, Tg and cyt C, yielded stable dispersions in PBS, while they caused precipitation in Milli-Q water. Why the NPs agglomerate in the case of Pep, but form stable dispersions with Ova, BSA and BLG, although these proteins are all negatively charged in Milli-Q and PBS, is unclear. But, it becomes obvious that the *protein identity* and the *environmental identity* of the system are significant parameters for the colloidal stability of the resulting NPs.

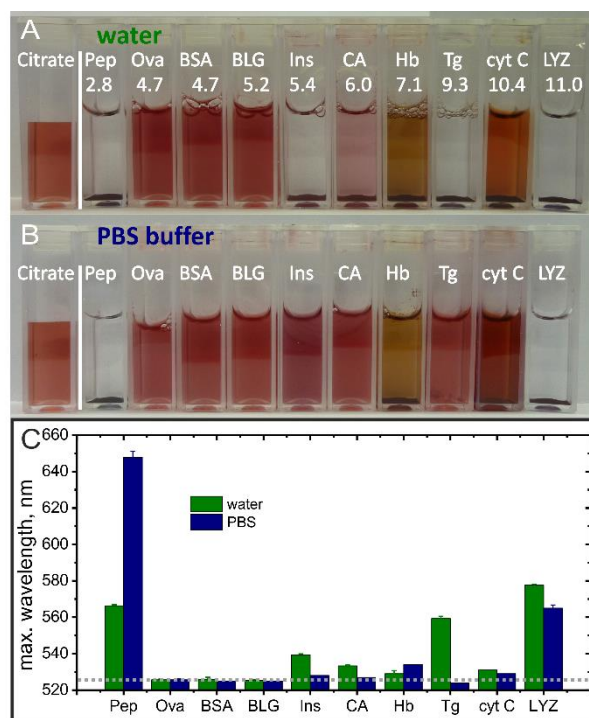


Figure 1: Functionalization of Au@Citrate by protein adsorption resulting in Au@Protein NPs. The photographs show the resulting protein-gold NP mixtures (A) in water (pH 5-6) and (B) in PBS buffer (pH 7.4), respectively, 24 h after mixing protein solution with Au@Citrate NPs. The vials in (A) and (B) are arranged according to the isoelectric point of the proteins⁴⁸⁻⁵³ increasing from left to right. (C) LSPR peak shifts of Au NPs dispersions (shaked) 24 h after mixing with proteins. The value of 520 nm corresponds to LSPR maximum of the original Au@Citrate NPs. The dotted grey line indicates the LSPR maximum value for the stable protein coated NPs. The shift of 3-4 nm was caused by refractive index changes, due to protein coating.

We studied the influence of the pH on the colloidal stability of NPs when they were exposed to proteins of different pI as shown in **Figure 2**. The pH of the protein solutions was adjusted to three different pH values, namely highly acidic, neutral and highly basic, and mixed with Au@Citrate NPs, giving final pH values of pH 2, pH 7 and pH 12, respectively. As shown in **Figure 2A, B** and **C**, the Au NP dispersions exhibited different colors and precipitation behavior depending on the protein and the environmental pH.

Mixing Au@Citrate NPs with Proteins:

At pH 2 (**Figure 2A** and red bars in **Figure 2D, E** and **F**), all investigated proteins were positively charged (all pI>2). Upon fast addition of Au@Citrate NPs to the acidic protein solutions, stable protein coated NPs were obtained for all proteins except for Pep and Ins (**Figure 2A**), which was surprising. The fact that the colloidal stability of the Au NPs is not affected during the coating process at pH 2, although the citrate molecules should be fully protonated and uncharged at this pH, and also the initially negatively charged Au@Citrate NPs do not aggregate with most of the positively charged proteins upon contact suggests fast protein adsorption on the particle surface with full coverage⁵⁴ and rapid charge inversion (**Figure 2F**). Please note that stable LYZ coated gold NPs (Au@LYZ) can be obtained by functionalizing the NPs at pH 2. To the best of our knowledge, this is the first time that stable LYZ coated NPs have been reported.¹⁷ In the case of Pep, the NPs agglomerate very strongly and precipitate completely in a short time (within ~ 3 hours). The LSPR exhibits a pronounced redshift of ca. 100 nm (**Figure 2D**) and the hydrodynamic size of the agglomerates reaches into the micron range (**Figure 2E**), making DLS measurements difficult (**Figure S2**). The reason for the NP agglomeration with Pep is likely to be the environmental pH in the reaction mixture, which is too close to the pI of pepsin (pI = 2.8). Pep

itself is not stable at this pH and therefore cannot stabilize the NPs. The ζ -potential of the final particles is around + 6 mV, which is not enough to stabilize the NPs (**Figure 2F**). Ins on the other hand induces NP agglomeration even though it is sufficiently positively charged at pH 2. The final agglomerates are small in size ($\sim 43 \pm 1$ nm), with a weak LSPR shift; they bear sufficient surface charges and are therefore stable over longer time periods (several days). The reason for the agglomeration with insulin at this pH is most probably the molecular weight of insulin (MW ~ 5.8 kDa⁵¹), which is low in comparison to the other investigated proteins. This result is consistent with our previous report on Ins-coated NPs.²⁸

At pH 7 (**Figure 2B** and green bars in **Figure 2D, E** and **F**), the colloidal stability behavior of the NPs can be divided into two groups. Proteins with $pI < 7$ result in stable Au@Protein NPs, whereas agglomeration is observed for proteins with $pI \geq pH$ 7 NP. Pep, a very low- pI protein, is an exception and leads to NP agglomeration. The NPs agglomerated weakly in the presence of Pep, which lead to a color change to purple (**Figure 2B**) and an LSPR redshift of only ca. 20 nm (**Figure 2D**). The agglomerates were in the size range of 50-60 nm (**Figure 2E**) with a negative ζ -potential of around - 20 mV (**Figure 2F**, green). Small agglomerate sizes and relatively high surface charge make these agglomerates stable over time; they do not precipitate for several days. Please note that in the presence of salt or at lower pH values the NPs agglomerate stronger and precipitate (**Figure 1**). Weakly acidic pI proteins ($4.5 \geq pI \leq 7$) such as Ova, BSA, BLG and Ins yielded stable NPs at pH 7, which is far enough from the protein pI s. The resulting Au@Protein NPs bear sufficient surface charge at this pH (**Figure 2F**, green) and therefore remain stable. Another exception are CA-coated gold NPs at pH 7. Due to the proximity of the pI of CA (6.0-6.6)⁵⁵⁻⁵⁶ to pH 7, the surface charge of the particles is around -10 mV (**Figure 2F**), which is below the stability threshold of (± 25 mV). Nevertheless, the particles remained stable even after 24 h incubation time according to UV-Vis and DLS data (**Figure 2D-E**). The reason for the stability of NPs with CA at this pH is most probably the high molecular weight of CA (MW = 77.8 kDa)⁵⁶, which provides steric stabilization to the coated NPs. Neutral- pI (Hb, $pI \sim 6.6-7.4$)^{49, 51-52} and high- pI proteins ($pI > 9$) such as Tg, cyt C and LYZ caused the NPs to agglomerate and sediment completely.

For Hb (pI ~ 6.6-7.4)^{49, 51-52}, the NPs agglomerated fast, probably due to the strong hydrophobic interactions of the protein at this pH that is close to its pI. With Tg, cyt C and LYZ, the NPs agglomerated and precipitated as well, probably due to Coulomb attraction between the positively charged proteins and the negatively charged Au@Citrate NPs at pH 7. The ζ -potential of the NPs was within the range of -10 to 0 mV (**Figure 2F**), which is insufficient to electrostatically stabilize the protein coated NPs.

At pH 12 (**Figure 2C** and blue bars in **Figure 2D, E** and **F**), the general trend is towards stable Au@Protein NPs. All the proteins were negatively charged at pH 12 and therefore compatible to the negatively charged Au@Citrate NPs in terms of surface charge. The proteins adsorbed onto the NPs without inducing Coulomb attraction and agglomeration.

We assume that there are two sources of agglomeration during the mixing of gold NPs with proteins that correlate with the pH of the mixture: 1) the insolubility of the excess protein and 2) the instability of the resulting Au@Protein NPs. The first case occurs if the environmental pH is close to pI of excess protein. The second case occurs if the pH is close to pI of the resulting Au@Protein system that differs from that of pure protein. It is known from literature (Au@BSA²⁷, Au@Ins²⁸) that the pI of a protein shifts upon adsorption onto gold NPs. If one of the two components that coexist in the mixture (Au@Protein or excess protein) has a pI close to the environmental pH, the entire dispersion agglomerates and sediments. For example, the pI of Au@Pep formed at pH 2 was shifted to ~5.5 from the pI (Pep) ~2.8⁴⁸ (**Figure 4**). The Au@NPs themselves were actually stable in pH 2 (**Figure 4A**) and should not agglomerate. The bad solubility and the high concentration of the excess protein with a pI close to pH 2 caused flocculation and removed the stable gold NPs from the dispersion, corresponding to the first case. An example for the second case is the functionalization of gold NPs with Pep at pH 7 (**Figure 2B**). In this case, the protein Pep is highly soluble at pH 7, however the Au@Pep NPs are unstable at pH 7 with ζ -potentials between 0 - 10 mV, which are below the stability threshold (**Figure 4A, E**). The high protein concentrations in our experiments largely suppressed contact between the NPs and protein-

induced bridging.⁴⁰ Bridging aggregation would prevent redispersion of Au@Pep NPs from agglomerates (formed at pH 2) via purification (in pH 12) (**Figure 3A, E-G**).

Surprisingly, dispersions formed with LYZ at pH 12 were stable over time, although the pH is close to the pI of LYZ (~ 11)^{50, 57} (**Figure 2C**). The surface charge of the LYZ-coated NPs at pH 12 was high enough to provide colloidal stability. A weak redshift of the LSPR peak for dispersions containing LYZ, BSA and Tg (**Figure 2D**) at pH 12 indicates a weak

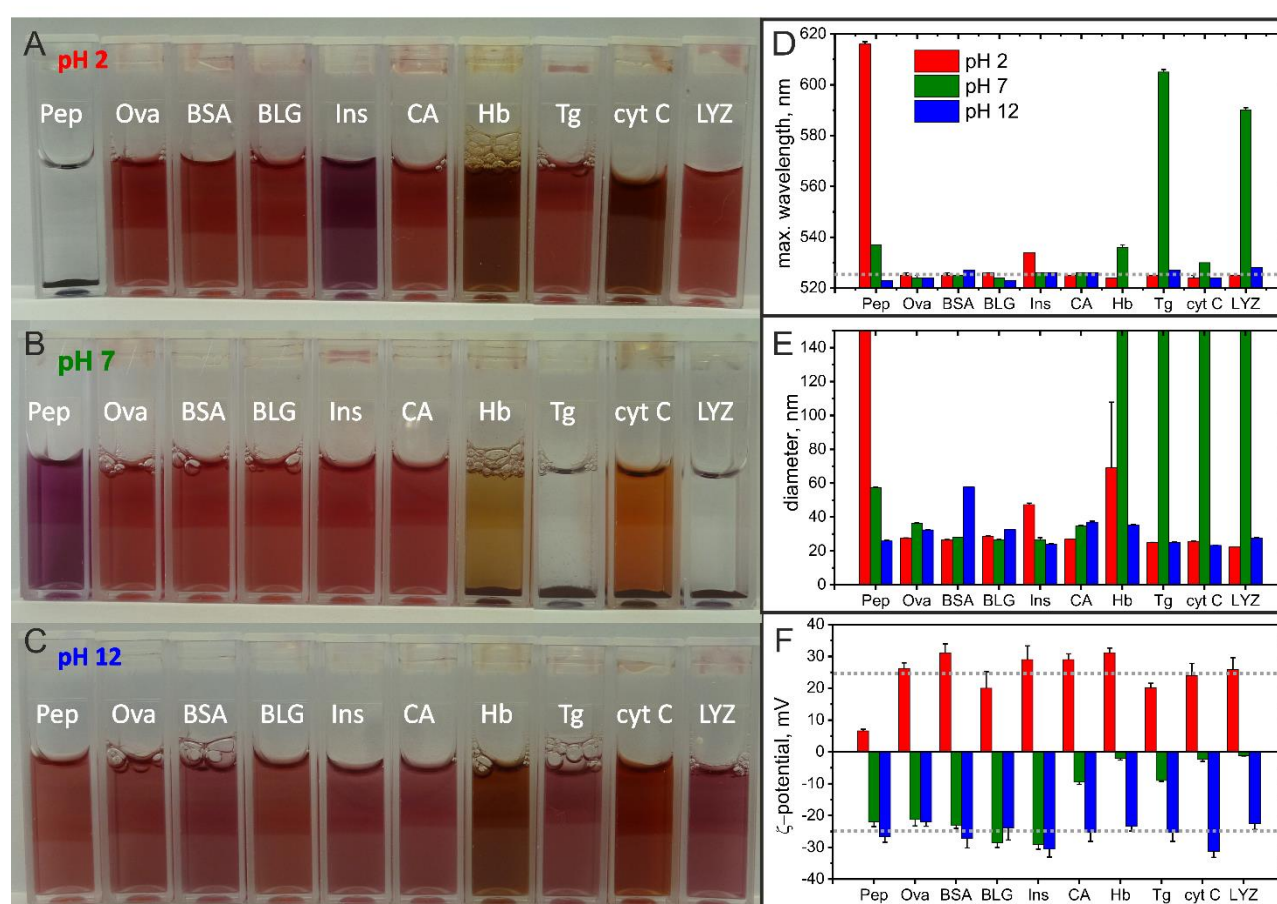


Figure 2: Functionalization of Au@Citrate by protein adsorption at different pH resulting in Au@Protein NPs of different stability. The images show the resulting protein-gold NP mixtures after 24 hours at A) pH 2, B) pH 7, and C) pH 12, respectively. The order of the cuvettes corresponds to an increasing isoelectric point of the proteins. The bar charts show the corresponding data of the D) LSPR peak, E) the hydrodynamic diameter (see Figure S2) and F) ζ -potential of these systems. The color code corresponds to the pH (red = pH 2, green = pH 7, blue = pH 12) and the dotted grey lines represent the stability thresholds (UV-Vis: 525 nm, ζ -potential: ± 25 mV).

agglomeration of NPs. These small agglomerates did not precipitate over time and were redispersed upon purification. Purification conditions, in particular the pH of the purification

media, are critical for the colloidal stability of the Au@Protein NPs and therefore, their impact was studied systematically in the following:

Purification of Au NPs after Protein Adsorption:

After mixing the NPs with proteins at different pH, the dispersions were washed three times with water at acidic, neutral and basic pH values via centrifugation and redispersion (see Experimental Section). The behavior of Au@Protein NPs after purification conditions is shown in **Figure 3**. We studied four different Au@Protein NP systems with a protein from each pI regime: low pI (Pep), intermediate pI (BLG) and high pI (LYZ). We studied Ins as a low molecular weight protein with an intermediate pI to assess the effect of the molecular weight when keeping the pI similar (Ins: pI 5.3,⁵⁸ MW 5.8 kDa, and BLG: pI 5.2,⁴⁹ MW 18.4 kDa).

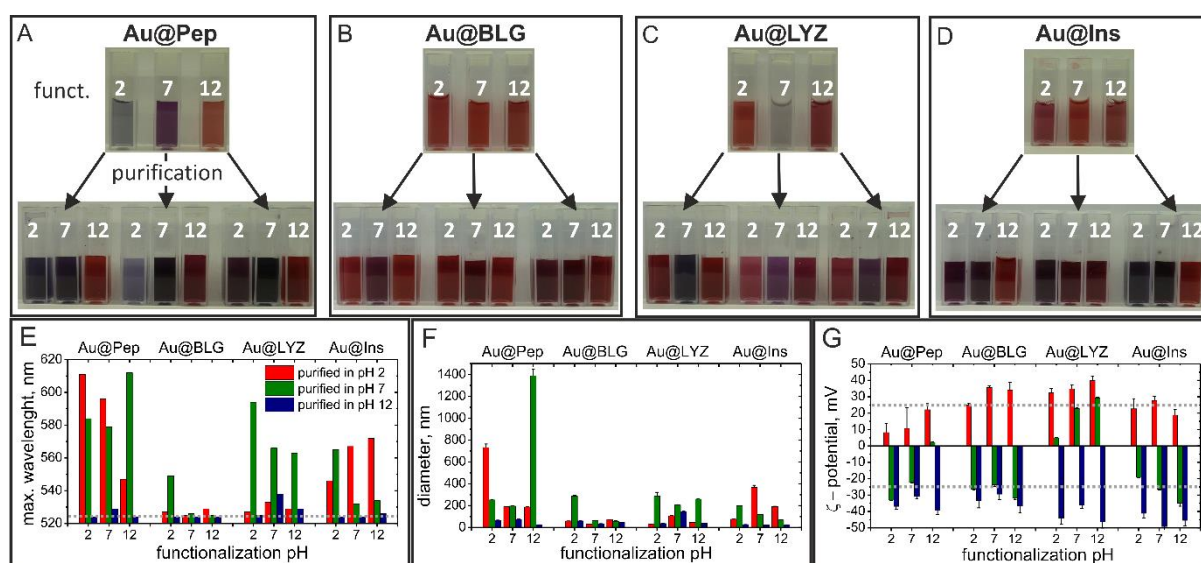


Figure 3: Purification can reverse NP agglomeration during the protein functionalization. Au@Citrate functionalized with Pep (A), BLG (B) LYZ (C) and Ins (D) at pH 2, 7 and 12 were purified at 3 different pH values. NPs that agglomerated during the functionalization (grey/blue and purple dispersions) were redispersed to individual NPs and regained their colloidal stability as indicated by the red color when purified at the right pH. The dotted grey lines (E, G) represent the stability thresholds (UV-Vis: 525 nm, ζ -potential: ± 25 mV).

The purified Au@Protein NP dispersions exhibited different stability behavior depending on the purification conditions, clearly seen by the different colors and LSPR shifts of the dispersions (**Figure A-E**). The Au@Pep system was only stable at pH 12, both during

functionalization and purification (Pep and Au@Pep are both stable at pH 12). Remarkably, the NP dispersions that were not stable and aggregated during the functionalization at pH 2 and 7 were redispersed completely upon purification at pH 12 as evidenced by UV-Vis and DLS measurements (**Figure 3E and F**). At pH 7, the purified Au@Pep NPs were not stable. At pH 2, the Au@Pep NPs became stable with increasing incubation time at this pH only when the NPs had been functionalized with Pep at pH 12 (see also **Figure 4A** and SI **Figure S3**).

The Au@BLG system (with intermediate pI) was functionalized (**Figure 2**) and purified at all three pH values (**Figure 3**) without affecting the colloidal stability of the dispersions. Only in the case of dispersions functionalized at pH 2 and purified at pH 7 did the NPs agglomerate upon purification as seen by the purple color of the dispersion and proven by UV-Vis and DLS. All three selected pH values (i.e. pH 2, 7 and 12) appear to be far enough from the pI of BLG and render Au@Protein NP systems stable.

The Au@LYZ system was functionalized at pH 2 (**Figure 2**) and then purified at pH 2 and pH 12 without destabilizing the NPs (**Figure 3**). At pH 7, the Au@LYZ NPs were unstable during both functionalization and purification. The NPs disaggregated to a certain extent when purified at pH 2 or 12, but not entirely, as indicated by plasmon peak shift (UV-Vis) and DLS. When functionalized at pH 12, Au@LYZ showed slight aggregation with a small redshift of the plasmon peak (**Figure 2**) that remained when purified at pH 2 and pH 12 and increased when purified at pH 7.

The Au@Ins system was functionalized at pH 7 and 12, but could only be purified and completely redispersed at pH 12. At pH 7, the NPs did not fully redisperse during purification (**Figure 3E and F**). At pH 2, the Au@Ins NPs were not stable at all, which is consistent with previous studies.²⁸ The ζ -potentials for Au@Ins NPs at pH 2 are not high enough to electrostatically stabilize the NPs. Ins also is smaller than BLG (or BSA²⁷) that does not provide additional steric stabilization to the NPs. Although the pI of the Ins and BLG is

similar, there are clear differences in their stability behavior, most likely due to the differences in their molecular weights.

It is worth noting that all Au NPs that agglomerated when mixed with proteins (**Figure 2A, B and C**), were fully recovered and stabilized again by purifying the agglomerated NPs at pH values far from the pI of the respective protein system (**Figure 3**). This indicates that when NPs meet proteins, reversible agglomeration can occur, which can be easily reversed. In general, for all protein systems investigated in this study, stable Au@Protein systems were obtained when functionalization was done at pH values far from pI of the proteins. The same trend existed for the purification of the NPs. However, the pH conditions for the functionalization step can also be different from that for purification. For example, for Au@LYZ, pH 2 was the optimum pH for functionalization, but pH 12 was optimal for purification. Surprisingly, pH 7 was not optimal for purification for the four Au@Protein systems (**Figure 3**). Hence, the pH of the dispersions had a huge impact on the final stability of the Au@Protein dispersions.

pH-dependent Colloidal Stability of Different Au@Protein NPs:

To understand the effect of the environmental pH on the stability of the different Au@Protein NPs, we studied the pH-dependent colloidal stability profiles for Au@Pep, Au@BLG, Au@LYZ and Au@Ins (**Figure 4**) over the pH range between pH 2 to 12, covering also a broad pI and MW range of proteins from acidic (Pep: 2.8)⁴⁸ to basic (LYZ: 11.0)^{50, 57} and from 5.8 kDa (Ins)⁵¹ to 34.6 kDa (Pep)⁵⁹, respectively. The NPs were functionalized with the proteins under the conditions that lead to the most stable Au@Protein NPs, i.e. Au@Pep in pH 12, Au@LYZ in pH 2; Au@BLG and Au@Ins in pH7. The stability profiles were assessed by measuring the LSPR shifts and ζ -potentials at different pH values. Furthermore, since the colloidal stability of Au@Protein NPs strongly depends on the surface charge of the NPs and thus, on the pH of the medium and the pI of the protein, the direction of the pH change played a significant role in the stability of the NPs and the redispersibility of their agglomerates. Moving from basic pH (pH 12), where all Au@Protein NPs were stable, to

acidic pH, the NPs started aggregating at neutral pH values and did not redisperse at extreme acidic pH values. Coming from acidic pH (pH 2) however, where the Au@Protein NPs were stable too (except Au@Ins), the NPs aggregated at neutral pH values, but redispersed completely at pH 12. To better understand the effect of pH and the direction of pH changes, we investigated the colloidal stability behavior of the four Au@Protein systems from both directions. Therefore, each system was purified in pH 2 and pH 12, setting the starting pH.

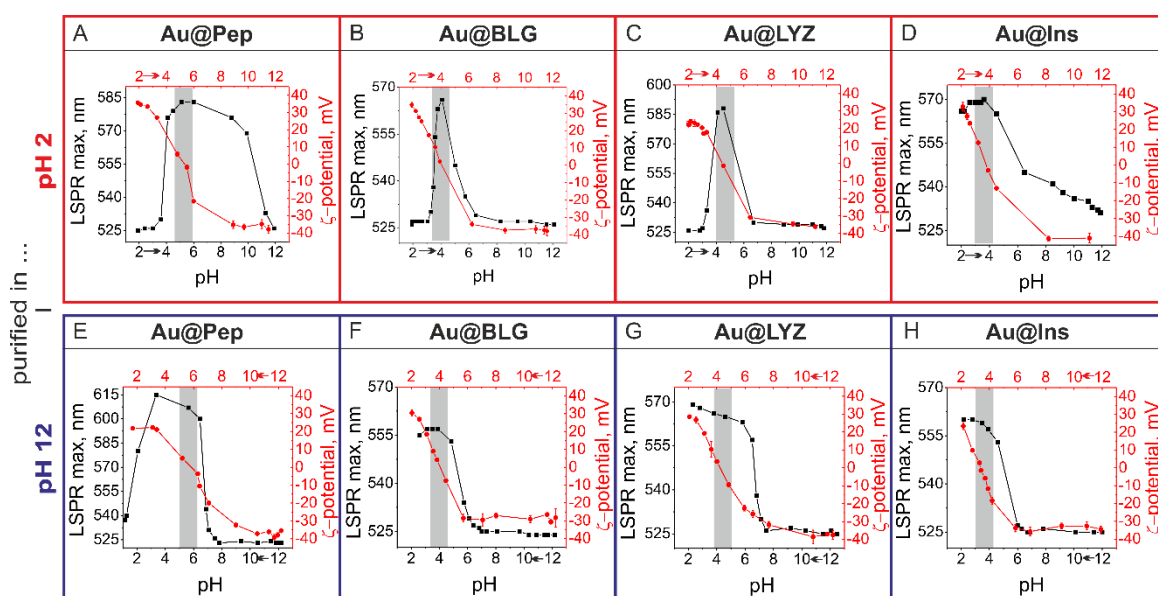


Figure 4: The effect of the pH of the purification medium on the pH stability range of the Au@Protein NPs. Au@Pep, Au@BLG, Au@Ins and Au@LYZ were functionalized under stable conditions and purified in pH 2 and pH 12, respectively. The pI of the Au@Protein NPs and the pH stability range of the NPs were determined by measuring the ζ -potential (red) and LSPR maximum, λ_{\max} (black) and as a function of solution pH. The grey stripes indicate the region of the pI of the respective Au@protein system (± 0.5 pH units).

In systems purified at pH 2, Au@Pep, Au@BLG and Au@LYZ were stable with the LSPR peak around 525 nm and ζ -potentials $\geq +30$ mV. Although they exhibit a ζ -potential of $\sim +30$ mV, the Au@Ins NPs were in an aggregated state with an LSPR peak beyond 565 nm, which has also been reported before.²⁸ The pH of the dispersions was then increased stepwise from pH 2. The surface charge of the Au@Protein NPs decreased from values well below +25 mV to zero, favoring hydrophobic interactions and leading to agglomeration of the Au@Pep (**Figure S4**), Au@BLG (**Figure S5**), Au@LYZ (**Figure S6**) and Au@Ins (**Figure**

S7) systems. The agglomeration caused their color to change from ruby red to blue/grey (**Figure S4-S7**). Further pH increase above the pI of Au@Protein NPs lead to charge inversion due to deprotonation of carboxyl and amino groups and to an increase of negatively charged groups. The ζ -potential of the NPs decreased below the stability threshold of -25 mV and the electrostatic repulsion between charged NPs increased, leading to complete redispersion of the NPs (LSPR \sim 525 nm). The three protein systems Au@Pep, Au@BLG and Au@LYZ exhibited U-shape stability profiles and were stable in both acidic and basic conditions. The Au@BLG and Au@LYZ showed a sharp transition between stable and unstable regime; the Au@Pep system showed a much broader instability regime. Although the ζ -potential values were beyond -25 mV at pH 8-9, the system fully recovered its LSPR peak only at pH 12. The disaggregation of the Au@Pep NPs was much slower than that of Au@BLG and Au@LYZ. A different stability behavior was observed for Au@Ins system. Increase of the pH caused charge inversion of this aggregated dispersion (**Figure 4D**), but redispersion was possible only at highly basic pH values.

All Au@Protein systems purified at pH 12 (**Figure 4E-H**) were highly stable with negative surface charges beyond -30 mV and LSPR absorption maxima at 525 nm. Upon decreasing the pH, the particles remained stable up to pH 7, and the LSPR maximum remained at 525 nm (**Figure 4E-H**). The ζ -potentials of the NPs also remained beyond -30 mV until pH 7. Only Au@Pep showed an increase of ζ -potential to -20 mV, but remained stable. Further pH decrease (pH < 7) caused all Au@Protein systems to start agglomerating and the LSPR peaks to shift to higher wavelengths. The NPs crossed the point of zero charge and inverted their surface charge to positive ζ -potentials. Only the Au@Pep system redispersed to great extent at pH values below pH 2 and the LSPR maximum recovered from 620 to 538 nm. The other three protein systems did not redisperse at acidic pH values (pH 2), although the surface charges reached high positive values beyond +30 mV. The pH-dependent stability of Au@Protein NPs strongly depended on the purification medium: the same Au@Protein systems (**Figure 4**) purified in different pH values, i.e. acidic (**Figure 4A-D**) and basic (**Figure 4E-H**), behaved entirely different.

The Au@BLG and Au@LYZ systems showed a pronounced influence of the purification pH on their colloidal stability behavior. Both NP systems were functionalized at optimal pH, i.e. Au@BLG at pH7 and Au@LYZ at pH 2. When the NPs were purified at acidic pH (**Figure 4B** and **C**), they exhibited a U-shaped pH stability profile that was similar to the bare proteins. The NPs were stable at pH values far below and above the pI of the Au@Protein system and unstable at pH close to pI. When the dispersions were purified at basic pH, the NPs were stable at pH values above the pI, but unstable at pH values below the pI, exhibiting a sigmoidal stability profile (**Figure 4F** and **G**). This pH dependent stability profile was confirmed via DLS and Cryo-TEM measurements, which is shown exemplarily for the Au@LYZ system in **Figure 5** (and for the Au@BLG system **Figure S8**). The Au@LYZ system was synthesized in pH 2 and purified in pH 2 (**Figure 5A-D**) and pH 12 (**Figure 5E-H**), yielding stable Au@LYZ NP dispersions of ruby red color and hydrodynamic sizes around 23 ± 0.3 nm. The Cryo-TEM images confirmed individually dispersed NPs for both cases (pH 2, **Figure 5B**, and pH 12 **Figure 5F**). When increasing or decreasing the pH towards the pI of the Au@LYZ system (i.e. ~ 4.3), the NPs started to agglomerate as seen from the color of the dispersion (purple, blue, grey). The hydrodynamic size of the agglomerates started increasing from hundreds of nanometers to micrometers. Loose flocs and 3D networks of NP agglomerates formed (**Figure 5C** and **G**). **Figure 4** illustrates how the Au@LYZ NPs behave differently for the two systems. When purified at pH 2, the agglomerates redispersed again to individual NPs (**Figure 5A** and **D**) at basic pH values. When purified at pH 12, the NP agglomerates formed at pH = pI that grew in size and density (**Figure 5E** and **H**) upon further pH decrease down to pH 2.

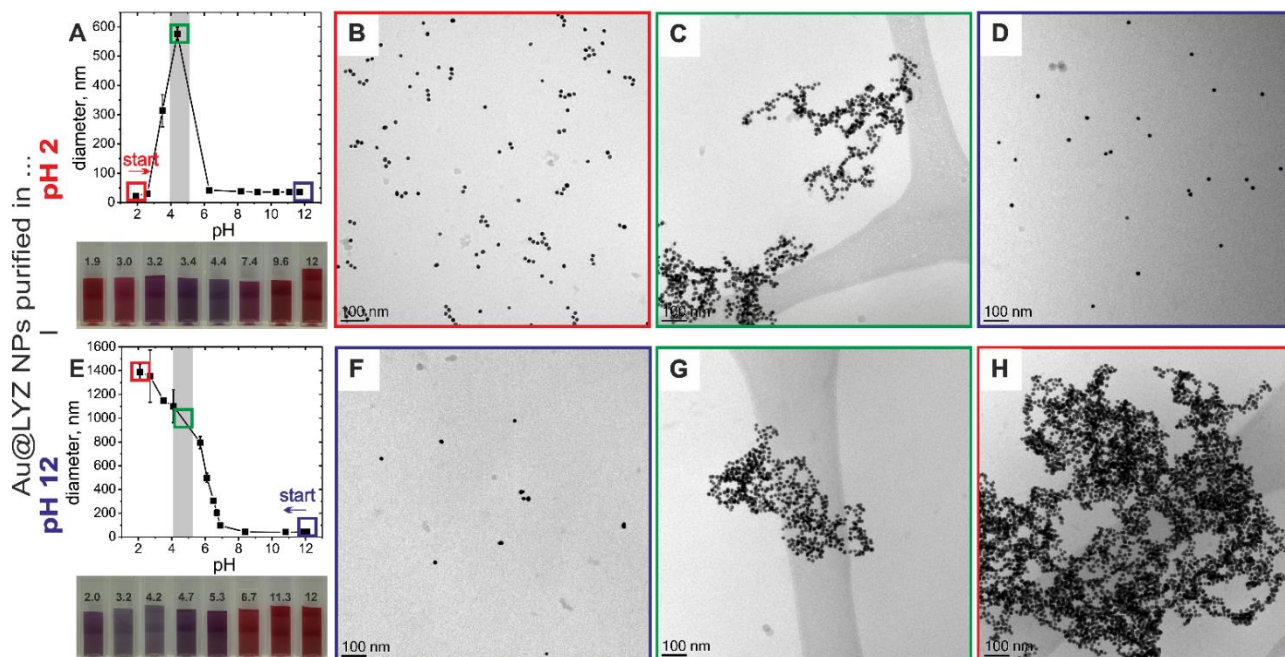


Figure 5: pH-dependent agglomeration behavior of colloidally stable Au@LYZ NPs purified at pH 2 (A-D) and pH 12 (E-H) measured with dynamic light scattering (A, E) and Cryo-TEM (B-D and F-H). Starting at pH 2, the Au@LYZ NPs are red in color and individually dispersed with small hydrodynamic sizes (A: red box), confirmed with Cryo-TEM (B). When increasing the pH, the NPs aggregated at the pI of Au@LYZ (A: green box, and C) and redispersed at pH 12 (A: blue box, and D). Starting at pH 12, the Au@LYZ NPs were red in color and individually dispersed with small hydrodynamic sizes (E: blue box), confirmed with Cryo-TEM (F). When decreasing the pH, the NPs aggregated at the pI of Au@LYZ (E: green box, and G) and aggregate further to bigger aggregates at pH 2 (E: red box, and H).

Au@Pep and Au@Ins systems showed similar profiles for both purification pH. The Au@Pep system showed a U-shaped stability profile, with a large instability range (> 6 pH units) in the medium pH region, slightly shifted, depending on the direction of the pH change. The Au@Ins system exhibited a sigmoidal-shaped stability profile for both cases, being stable at basic pH values and unstable at acidic pH values.

These differences in the stability profiles of the Au@Protein NPs are surprising for different purification conditions, although the NPs, the proteins and the synthesis conditions (coating procedure) are the same. The Au@Protein NPs behave different from the pure proteins. Bare proteins usually exhibit a U-shaped solubility profile with high solubility at pH values below and above the pI and a low solubility at pH = pI. The pI of proteins depends on the ratio of the negatively and positively charged amino acid residues. When proteins adsorb or

bind onto metal surfaces, they may bind with both negatively or positively charged functional groups, which become then unavailable for the interactions with outer medium, i.e. water. The ratio between these charged groups changes upon binding, which leads to a measurable shift in pI. Depending on the functional groups that are available on the protein and bind to the gold surface, the pI can be shifted towards lower or higher pH values compared to the original pI of the protein. When a protein binds to the NP with basic (positively charged) groups, such as amino, imidazole or guanidino groups, the pI of the resulting Au@Protein system shifts to lower pH values. If the protein binds with the carboxylic (negatively charged) groups to the surface, the pI shift is expected to be towards higher pH values. In the case of NPs being coated with BLG, Ins and LYZ, the pI shifted towards lower pH values. We assume that these proteins adsorb onto gold surfaces, preferentially via basic groups. The pI of Au@Protein systems containing proteins with intermediate proteins, such as Au@BLG and Au@Ins, was measured to be 4.1 (BLG: 5.2⁴⁹) and 3.5 (Ins: 5.3⁵⁸), which is consistent with literature²⁷⁻²⁸. High-pI proteins such as LYZ (pI: 11.0^{50, 57}) exhibited a pronounced pI shift towards pH ~ 4.3) when adsorbed on to the Au NPs. This suggests that the main binding groups also for Au@LYZ are the basic functional groups. In contrast, the low-pI protein pepsin (2.8⁴⁸) exhibits a pI shift to higher pH values with a pI~ 5.5. This indicates that pepsin binds to the gold NP surface to a larger part via carboxyl groups, which are indeed abundant in the protein. Furthermore, pepsin has relatively low amount of positively charged groups (4 in total, i.e. 2 Arg, 1 His, 1 Lys).⁵⁹⁻⁶⁰ Nevertheless, it is remarkable that the pI-shifts for all Au@Protein systems investigated in this study were independent of the purification medium (pH 2 or 12, see **Figure 4**). In fact, this behavior is plausible, since the proteins were adsorbed (functionalization step) under same conditions. Hence, we assume that protein adsorption occurred onto gold surface via same sites, leaving same functional groups available towards the solvent (water). Consequently, this would lead to the same final pI of an Au@Protein system, which is independent of the purification conditions.

The proteins' molecular weight also affects the stability of Au@Protein. Proteins with high molecular weight contribute to the stability of the proteins coated NPs with steric stabilization additional to the electrostatic stabilization.²⁶⁻²⁷ From the four investigated proteins, Ins with its 5.8 kDa⁵¹ molecular weight is the smallest (<10000), BLG (18.4 kDa⁴⁹) and LYZ (14.3 kDa^{50, 61}) are in the middle range, and Pep (34.6 kDa⁵⁹) is the largest. Large proteins have many acidic and basic functional groups that probably provide enough electrostatic repulsion on the Au@Protein surface upon pH change. Additionally, their size provides steric repulsion. The Au@Pep system's U-shaped stability profile can be attributed to the electrosteric stabilization mechanism. Smaller proteins have less functional groups and provide less steric repulsion. The Au@Ins system for example is stable at basic pH but unstable at acidic pH independent of the purification pH. Insulin is a very small protein and cannot provide steric repulsion to disagglomerate the system completely. In the case of the middle-sized proteins, both Au@BLG and Au@LYZ systems are sensitive to the direction of pH change, however it is not clear yet what causes the direction-dependent stabilities of the systems.

Remarkably, the stability profiles of all Au@Protein systems were highly consistent over multiple aggregation/disaggregation cycles. **Figure 6** shows three-point pH switching cycles for all four protein coated NP systems purified at pH 2 and pH 12, in analogy to **Figure 4**. The purification pH served as starting point as shown in **Figure 6**. The reversible agglomeration and disagglomeration was followed by recording the LSPR peak maximum of the dispersions at different pH values via UV-Vis spectroscopy. All Au@Protein systems maintained their original stability profiles (**Figure 4**) at least over three pH cycles. For example, Au@Pep (both purification pH, **Figure 6A** and **E**) and Au@BLG and Au@LYZ (pH 2 purification, **Figure 6B** and **C**) were highly stable at extreme pH values and aggregated at pH = pI (U-shaped profile), recovering completely after each cycle. Upon a sudden pH change from one extreme to other extreme pH, e.g. from pH 12 to pH 2 (**Figure 6A-C** and **E**, at the end of a cycle) the particles remained stable. The reason for this is that the pH change is fast and the particles undergo an immediate charge inversion, without agglomerating, while going through the point of zero charge. Au@Ins (**Figure 6D** and **H**) and Au@BLG and

Au@LYZ (pH 12 purification, **Figure 6F and G**) on the other hand, exhibited sigmoidal stability profiles, being stable only at basic pH values, in analogy to **Figure 4**.

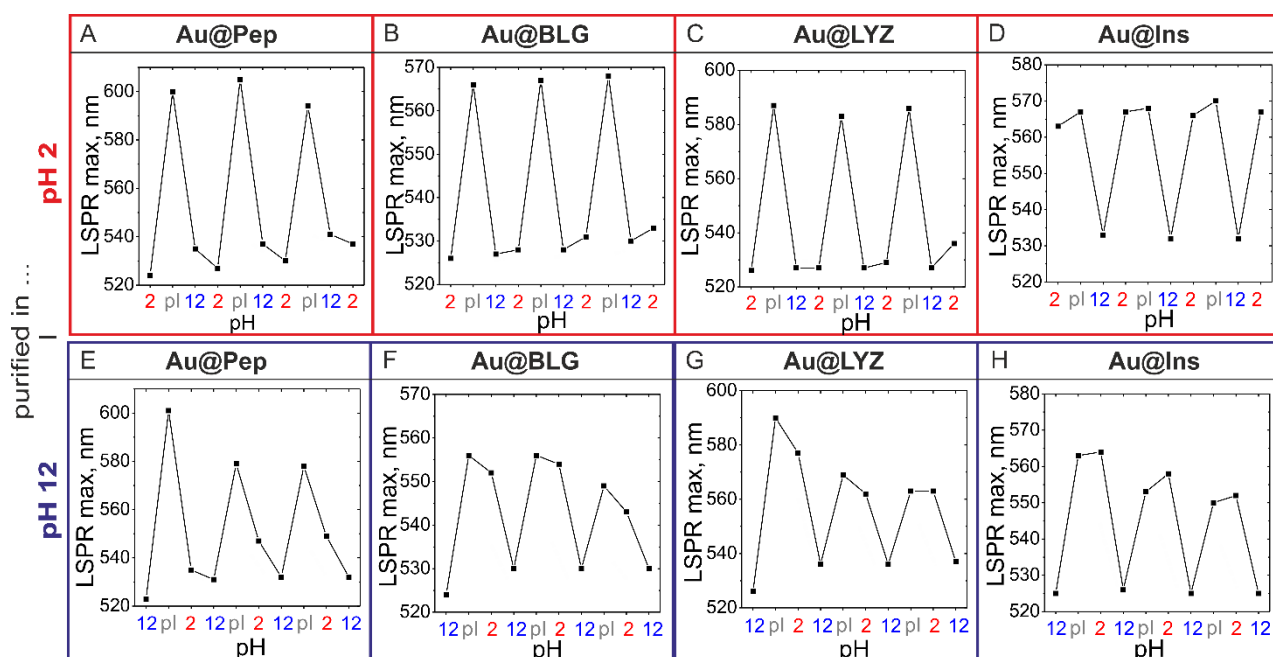


Figure 6: pH-responsive reversible aggregation-disaggregation cycles of four representative protein coated gold NPs. The Au@Pep (A, E), Au@BLG (B, F), Au@LYZ (C, G) and Au@Ins (D, H) NPs were functionalized under stable conditions and purified in pH 2 (A-D) and pH 12 (E-H). The pH of the dispersions was changed from pH 2 to pH 12 (A-D) or vice versa (E-H) going over the pI of the protein coated NPs. The reversible aggregation of the different Au@Protein NPs was followed via UV-Vis spectroscopy, by measuring the LSPR maximum λ_{\max} .

Conclusion

The behavior of Au@Protein dispersions strongly depends on three parameters: a) *nanoparticle identity*, b) *protein identity* and c) *environmental identity*. The present study reveals the importance of the *protein identity* and the environmental conditions on the final physico-chemical properties of metal nanoparticle systems stabilized by small charged molecules such as citrate. The NPs either formed stable dispersions or agglomerated spontaneously when mixed with protein solutions, depending on the pI of the protein and pH

of the mixture. The agglomerates redispersed when purified under suitable conditions. The final Au@Protein NPs exhibited a stability regime and stability profile that strongly depended on the adsorbed protein and the environmental conditions. The surface charge of the Au@Protein NPs also depended on the pI and the pH. Controlling the environmental parameters and adjusting them to the physico-chemical properties of the proteins and of NPs allowed us to create highly stable Au@Protein NPs with a defined protein corona and thus, with a defined bio-interface. Understanding the interactions of nanomaterials with individual proteins in regard of their abundance, composition, and physico-chemical properties would allow us to decipher the formation of the new physico-chemical identity upon protein adsorption in complex biological systems and fluids.

Funding Sources

German Research Foundation (DFG) - SFB 840, German Federal Environmental Foundation (DBU)

Acknowledgements

This study was funded by the German Research Foundation (DFG) within the collaborative research center SFB 840. J.S. was supported and funded via a grant for PhD candidates of the German Federal Environmental Foundation (DBU). The authors would like to thank Markus Drechsler for Cryo-TEM, Carmen Kunert for TEM measurements and Corinna Link for proof reading. T.K. thanks Eduard Arzt for his continuing support. M.C. thanks Andreas Fery for his broad support and scientific discussions to this paper.

ASSOCIATED CONTENT

Supporting Information Description

TEM images of the Au@Citrate NPs, UV-Vis spectra of various Au@Protein NPs measured 24 hours after functionalization, and after purification at different pH values. This material is available free of charge via the Internet at <http://pubs.acs.org>.

REFERENCES

- (1) Walczyk, D.; Bombelli, F. B.; Monopoli, M. P.; Lynch, I.; Dawson, K. A., What the Cell "Sees" in Bionanoscience. *J. Am. Chem. Soc.* **2010**, *132*, 5761-5768.
- (2) Kelly, P. M.; Åberg, C.; Polo, E.; O'Connell, A.; Cookman, J.; Fallon, J.; Krpetić, Ž.; Dawson, K. A., Mapping Protein Binding Sites on the Biomolecular Corona of Nanoparticles. *Nat. Nano* **2015**, *10*, 472-479.
- (3) Lynch, I.; Dawson, K. A., Protein-Nanoparticle Interactions. *Nano Today* **2008**, *3*, 40-47.
- (4) Nel, A. E.; Madler, L.; Velegol, D.; Xia, T.; Hoek, E. M.; Somasundaran, P.; Klaessig, F.; Castranova, V.; Thompson, M., Understanding Biophysicochemical Interactions at the Nano-Bio Interface. *Nat. Mater.* **2009**, *8*, 543-57.
- (5) Yan, Y.; Gause, K. T.; Kamphuis, M. M. J.; Ang, C.-S.; O'Brien-Simpson, N. M.; Lenzo, J. C.; Reynolds, E. C.; Nice, E. C.; Caruso, F., Differential Roles of the Protein Corona in the Cellular Uptake of Nanoporous Polymer Particles by Monocyte and Macrophage Cell Lines. *ACS Nano* **2013**, *7*, 10960-10970.
- (6) Wei, Q.; Becherer, T.; Angioletti-Uberti, S.; Dzubiella, J.; Wischke, C.; Neffe, A. T.; Lendlein, A.; Ballauff, M.; Haag, R., Protein Interactions with Polymer Coatings and Biomaterials. *Angew. Chem. Int. Ed.* **2014**, *53*, 8004-8031.
- (7) Bertoli, F.; Davies, G.-L.; Monopoli, M. P.; Moloney, M.; Gun'ko, Y. K.; Salvati, A.; Dawson, K. A., Magnetic Nanoparticles to Recover Cellular Organelles and Study the Time Resolved Nanoparticle-Cell Interactome Throughout Uptake. *Small* **2014**, *10*, 3307-3315.
- (8) Zakaria, H. M.; Shah, A.; Konieczny, M.; Hoffmann, J. A.; Nijdam, A. J.; Reeves, M. E., Small Molecule- and Amino Acid-Induced Aggregation of Gold Nanoparticles. *Langmuir* **2013**, *29*, 7661-7673.
- (9) Chah, S.; Hammond, M. R.; Zare, R. N., Gold Nanoparticles as a Colorimetric Sensor for Protein Conformational Changes. *Chem. Biol.* **2005**, *12*, 323-328.
- (10) Pavlov, V.; Xiao, Y.; Shlyahovsky, B.; Willner, I., Aptamer-Functionalized Au Nanoparticles for the Amplified Optical Detection of Thrombin. *J. Am. Chem. Soc.* **2004**, *126*, 11768-11769.
- (11) Bhattacharya, J.; Jasrapuria, S.; Sarkar, T.; GhoshMoulick, R.; Dasgupta, A. K., Gold Nanoparticle-Based Tool to Study Protein Conformational Variants: Implications in Hemoglobinopathy. *Nanomed. Nanotechnol. Biol. Med.* **2007**, *3*, 14-19.
- (12) Wang, Z.; Lee, J.; Cossins, A. R.; Brust, M., Microarray-Based Detection of Protein Binding and Functionality by Gold Nanoparticle Probes. *Anal. Chem.* **2005**, *77*, 5770-5774.
- (13) Kerman, K.; Chikae, M.; Yamamura, S.; Tamiya, E., Gold Nanoparticle-Based Electrochemical Detection of Protein Phosphorylation. *Anal. Chim. Acta.* **2007**, *588*, 26-33.
- (14) Albanese, A.; Chan, W. C. W., Effect of Gold Nanoparticle Aggregation on Cell Uptake and Toxicity. *ACS Nano* **2011**, *5*, 5478-5489.
- (15) Ghosh, P.; Han, G.; De, M.; Kim, C. K.; Rotello, V. M., Gold Nanoparticles in Delivery Applications. *Adv. Drug Del. Rev.* **2008**, *60*, 1307-1315.
- (16) Duncan, B.; Kim, C.; Rotello, V. M., Gold Nanoparticle Platforms as Drug and Biomacromolecule Delivery Systems. *J. Control. Release* **2010**, *148*, 122-127.
- (17) Zhang, D. M.; Neumann, O.; Wang, H.; Yuwono, V. M.; Barhoumi, A.; Perham, M.; Hartgerink, J. D.; Wittung-Stafshede, P.; Halas, N. J., Gold Nanoparticles Can Induce the Formation of Protein-Based Aggregates at Physiological pH. *Nano Lett.* **2009**, *9*, 666-671.
- (18) Chen, Y. M.; Yu, C. J.; Cheng, T. L.; Tseng, W. L., Colorimetric Detection of Lysozyme Based on Electrostatic Interaction with Human Serum Albumin-Modified Gold Nanoparticles. *Langmuir* **2008**, *24*, 3654-3660.
- (19) Garabagiu, S., A Spectroscopic Study on the Interaction between Gold Nanoparticles and Hemoglobin. *Mater. Res. Bull.* **2011**, *46*, 2474-2477.
- (20) Horovitz, O.; Tomoiaia, G.; Mocanu, A.; Yupsanis, T.; Tomoiaia-Cotisel, M., Protein Binding to Gold Colloids. *Gold Bull.* **2007**, *40*, 213-218.

- (21) Lacerda, S. H. D. P.; Park, J. J.; Meuse, C.; Pristiniski, D.; Becker, M. L.; Karim, A.; Douglas, J. F., Interaction of Gold Nanoparticles with Common Human Blood Proteins. *ACS Nano* **2010**, *4*, 365-379.
- (22) Tom, R. T.; Pradeep, T., Interaction of Azide Ion with Hemin and Cytochrome C Immobilized on Au and Ag Nanoparticles. *Langmuir* **2005**, *21*, 11896-11902.
- (23) Thobhani, S.; Attree, S.; Boyd, R.; Kumarswami, N.; Noble, J.; Szymanski, M.; Porter, R. A., Bioconjugation and Characterisation of Gold Colloid-Labelled Proteins. *J. Immunol. Methods* **2010**, *356*, 60-69.
- (24) Yang, Y.; Burkhard, P., Encapsulation of Gold Nanoparticles into Self-Assembling Protein Nanoparticles. *J. Nanobiotechnol.* **2012**, *10*, 42-53.
- (25) Moerz, S. T.; Kraegeloh, A.; Chanana, M.; Kraus, T., Formation Mechanism for Stable Hybrid Clusters of Proteins and Nanoparticles. *ACS Nano* **2015**, *9*, 6696-6705.
- (26) Chanana, M.; Gil, P. R.; Correa-Duarte, M. A.; Liz-Marzan, L. M.; Parak, W. J., Physicochemical Properties of Protein-Coated Gold Nanoparticles in Biological Fluids and Cells before and after Proteolytic Digestion. *Angew. Chem. Int. Ed.* **2013**, *52*, 4179-4183.
- (27) Strozyk, M. S.; Chanana, M.; Pastoriza-Santos, I.; Perez-Juste, J.; Liz-Marzan, L. M., Protein/Polymer-Based Dual-Responsive Gold Nanoparticles with pH-Dependent Thermal Sensitivity. *Adv. Funct. Mater.* **2012**, *22*, 1436-1444.
- (28) Chanana, M.; Correa-Duarte, M. A.; Liz-Marzan, L. M., Insulin-Coated Gold Nanoparticles: A Plasmonic Device for Studying Metal-Protein Interactions. *Small* **2011**, *7*, 2650-2660.
- (29) Tebbe, M.; Kuttner, C.; Mannel, M.; Fery, A.; Chanana, M., Colloidally Stable and Surfactant-Free Protein-Coated Gold Nanorods in Biological Media. *ACS Appl. Mater. Interfaces* **2015**, *7*, 5984-91.
- (30) Rayavarapu, R. G.; Petersen, W.; Ungureanu, C.; Post, J. N.; van Leeuwen, T. G.; Manohar, S., Synthesis and Bioconjugation of Gold Nanoparticles as Potential Molecular Probes for Light-Based Imaging Techniques. *Int. J. Biomed. Imaging* **2007**, *2007*, 29817-29827.
- (31) Welsch, N.; Lu, Y.; Dzubiella, J.; Ballauff, M., Adsorption of Proteins to Functional Polymeric Nanoparticles. *Polymer* **2013**, *54*, 2835-2849.
- (32) Zustiak, S. P.; Wei, Y.; Leach, J. B., Protein-Hydrogel Interactions in Tissue Engineering: Mechanisms and Applications. *Tissue Eng. Part B Rev.* **2013**, *19*, 160-171.
- (33) Bharti, B.; Meissner, J.; Findenegg, G. H., Aggregation of Silica Nanoparticles Directed by Adsorption of Lysozyme. *Langmuir* **2011**, *27*, 9823-9833.
- (34) Schmidtke, C.; Lange, H.; Tran, H.; Ostermann, J.; Kloust, H.; Bastús, N. G.; Merkl, J.-P.; Thomsen, C.; Weller, H., Radical Initiated Reactions on Biocompatible Cdse-Based Quantum Dots: Ligand Cross-Linking, Crystal Annealing, and Fluorescence Enhancement. *J. Phys. Chem. C* **2013**, *117*, 8570-8578.
- (35) Ament, I.; Prasad, J.; Henkel, A.; Schmachtel, S.; Sonnichsen, C., Single Unlabeled Protein Detection on Individual Plasmonic Nanoparticles. *Nano Lett.* **2012**, *12*, 1092-1095.
- (36) Ahijado-Guzman, R.; Prasad, J.; Rosman, C.; Henkel, A.; Tome, L.; Schneider, D.; Rivas, G.; Sonnichsen, C., Plasmonic Nanosensors for Simultaneous Quantification of Multiple Protein-Protein Binding Affinities. *Nano Lett.* **2014**, *14*, 5528-5532.
- (37) Kinnear, C.; Dietsch, H.; Clift, M. J.; Endes, C.; Rothen-Rutishauser, B.; Petri-Fink, A., Gold Nanorods: Controlling Their Surface Chemistry and Complete Detoxification by a Two-Step Place Exchange. *Angew. Chem. Int. Ed.* **2013**, *52*, 1934-1938.
- (38) Mahmoudi, M.; Lohse, S. E.; Murphy, C. J.; Fathizadeh, A.; Montazeri, A.; Suslick, K. S., Variation of Protein Corona Composition of Gold Nanoparticles Following Plasmonic Heating. *Nano Lett.* **2014**, *14*, 6-12.
- (39) Turkevich, J.; Stevenson, P. C.; Hillier, J., A Study of the Nucleation and Growth Processes in the Synthesis of Colloidal Gold. *Discuss. Faraday Soc.* **1951**, 55-75.
- (40) Bharti, B.; Meissner, J.; Klapp, S. H.; Findenegg, G. H., Bridging Interactions of Proteins with Silica Nanoparticles: The Influence of pH, Ionic Strength and Protein Concentration. *Soft Matter* **2014**, *10*, 718-728.

- (41) Kuehner, D. E.; Engmann, J.; Fergg, F.; Wernick, M.; Blanch, H. W.; Prausnitz, J. M., Lysozyme Net Charge and Ion Binding in Concentrated Aqueous Electrolyte Solutions. *J. Phys. Chem. B* **1999**, *103*, 1368-1374.
- (42) Delahaije, R. J.; Wierenga, P. A.; van Nieuwenhuijzen, N. H.; Giuseppin, M. L.; Gruppen, H., Protein Concentration and Protein-Exposed Hydrophobicity as Dominant Parameters Determining the Flocculation of Protein-Stabilized Oil-in-Water Emulsions. *Langmuir* **2013**, *29*, 11567-11574.
- (43) Salis, A.; Bostrom, M.; Medda, L.; Cugia, F.; Barse, B.; Parsons, D. F.; Ninham, B. W.; Monduzzi, M., Measurements and Theoretical Interpretation of Points of Zero Charge/Potential of BSA Protein. *Langmuir* **2011**, *27*, 11597-11604.
- (44) Jachimska, B.; Pajor, A., Physico-Chemical Characterization of Bovine Serum Albumin in Solution and as Deposited on Surfaces. *Bioelectrochemistry* **2012**, *87*, 138-146.
- (45) Engelhardt, K.; Lexis, M.; Gochev, G.; Konnerth, C.; Miller, R.; Willenbacher, N.; Peukert, W.; Braunschweig, B., pH Effects on the Molecular Structure of Beta-Lactoglobulin Modified Air-Water Interfaces and Its Impact on Foam Rheology. *Langmuir* **2013**, *29*, 11646-11655.
- (46) Arakawa, T.; Timasheff, S. N., Mechanism of Protein Salting in and Salting out by Divalent Cation Salts: Balance between Hydration and Salt Binding. *Biochemistry* **1984**, *23*, 5912-5923.
- (47) Zhang, F.; Skoda, M. W. A.; Jacobs, R. M. J.; Martin, R. A.; Martin, C. M.; Schreiber, F., Protein Interactions Studied by SAXS: Effect of Ionic Strength and Protein Concentration for BSA in Aqueous Solutions. *J. Phys. Chem. B* **2007**, *111*, 251-259.
- (48) Malamud, D.; Drysdale, J. W., Isoelectric Points of Proteins: A Table. *Anal. Biochem.* **1978**, *86*, 620-647.
- (49) Righetti, P. G.; Caravaggio, T., Isoelectric Points and Molecular-Weights of Proteins - a Table. *J. Chromatogr.* **1976**, *127*, 1-28.
- (50) Lauer, H. H.; McManigill, D., Capillary Zone Electrophoresis of Proteins in Untreated Fused-Silica Tubing. *Anal. Chem.* **1986**, *58*, 166-170.
- (51) Ui, N., Isoelectric Points and Conformation of Proteins .1. Effect of Urea on Behavior of Some Proteins in Isoelectric Focusing. *Biochim. Biophys. Acta* **1971**, *229*, 567-581.
- (52) Righetti, P. G.; Tudor, G.; Ek, K., Isoelectric Points and Molecular-Weights of Proteins - a New Table. *J. Chromatogr.* **1981**, *220*, 115-194.
- (53) Walsh, K. A.; Neurath, H., Trypsinogen and Chymotrypsinogen as Homologous Proteins. *Proc. Natl. Acad. Sci. USA* **1964**, *52*, 884-889.
- (54) Casals, E.; Pfaller, T.; Duschl, A.; Oostingh, G. J.; Puentes, V., Time Evolution of the Nanoparticle Protein Corona. *ACS Nano* **2010**, *4*, 3623-3632.
- (55) Jeltsch, J. M.; Chambon, P., The Complete Nucleotide-Sequence of the Chicken Ovotransferrin Messenger-Rna. *Eur. J. Biochem.* **1982**, *122*, 291-295.
- (56) Williams, J.; Elleman, T. C.; Kingston, I. B.; Wilkins, A. G.; Kuhn, K. A., The Primary Structure of Hen Overtransferrin. *Eur. J. Biochem.* **1982**, *122*, 297-303.
- (57) Wetter, L. R.; Deutsch, H. F., Immunological Studies on Egg White Proteins. 4. Immunochemical and Physical Studies of Lysozyme. *J. Biol. Chem.* **1951**, *192*, 237-242.
- (58) Fischel-Ghodsian, F.; Brown, L.; Mathiowitz, E.; Brandenburg, D.; Langer, R., Enzymatically Controlled Drug Delivery. *Proc. Natl. Acad. Sci. USA* **1988**, *85*, 2403-2406.
- (59) Sepulveda, P.; Marciniszyn, J.; Liu, D.; Tang, J., Primary Structure of Porcine Pepsin. *J. Biol. Chem.* **1975**, *250*, 5082-5088.
- (60) Tang, J.; Sepulveda, P.; Marcinis, J.; Chen, K. C. S.; Huang, W. Y.; Tao, N.; Liu, D.; Lanier, J. P., Amino-Acid Sequence of Porcine Pepsin. *Proc. Natl. Acad. Sci. USA* **1973**, *70*, 3437-3439.
- (61) Canfield, R. E., Amino Acid Sequence of Egg White Lysozyme. *J. Biol. Chem.* **1963**, *238*, 2698-2707.

TOC Figure:

